

Biosynthesis of neocarazostatin A reveals the sequential carbazole prenylation and hydroxylation in the tailoring steps

Sheng Huang,¹ Somayah Sameer Elsayed,² Meinan Lv,¹ Jioji Tabudravu,² Mostafa E. Rateb,^{2,4} Roland Gyampoh,³ Kwaku Kyeremeh,³ Rainer Ebel,² Marcel Jaspars,² Zixin Deng,¹ Yi Yu,*¹ Hai Deng*²

1. Sheng, Huang; Meinan Lv; Zixin, Deng; Yi, Yu
Key Laboratory of Combinatory Biosynthesis and Drug Discovery (Ministry of Education),
School of Pharmaceutical Sciences,
Wuhan University,
185 East Lake Road, Wuhan 430071 P. R. China
E-mail: yu_yi@whu.edu.cn
2. Somayah, S. Elsayed; Jioji, Tabudravu; Mostafa, Rateb; Rainer, Ebel; Marcel Jaspars; Hai, Deng
Department of Chemistry
University of Aberdeen,
Aberdeen, AB24 3UE,
United Kingdom
E-mail: h.deng@abdn.ac.uk
3. Roland Gyampoh; Kwaku, Kyeremeh
Department of Chemistry
University of Ghana
P.O. Box LG56, Legon-Accra, Ghana
4. Pharmacognosy Department,
School of Pharmacy,
Beni-Suef University,
Beni-Suef 32514
Egypt

Running title: Biosynthesis of neocarazostatin A

Keywords: carbazole alkaloids, biosynthesis, prenyltransferase, reconstitution, P450 enzyme, neocarazostatin A

Summary

Neocarazostatin A (NZS) is a bacterial alkaloid with promising bioactivities against free radicals, featuring a tricyclic carbazole nucleus with a prenyl moiety at C-6 of the carbazole ring. Herein we report the discovery and characterization of the biosynthetic pathway of NZS through genome mining and gene inactivation. The *in vitro* assays characterized two enzymes: NzsA is a P450 hydroxylase and NzsG is a new phytoene-synthase-like prenyltransferase (PTase). This is the first reported native PTase that specifically acts on carbazole nucleus. Finally, our *in vitro* reconstituted experiment demonstrated a coupled reaction catalysed by NzsG and NzsA tailoring the NZS biosynthesis.

Introduction

Carbazoles consist of a tricyclic nucleus with two benzene rings flanking a pyrrole ring. Most of the known naturally occurring carbazole alkaloids contain an annulated ring or ring system in both benzene rings and were isolated from higher plants and fungi, which display a broad range of biological properties such as anticancer, antibacterial, antiviral, and antiplasmodial activities (Knölker and Reddy, 2002). To date, the biosynthesis of plant carbazole metabolites is not fully understood (Schmidt, et al., 2012). The most widely accepted hypothesis is that the nucleus of carbazole alkaloids from higher plants may derive from anthranilic acids and prenyl pyrophosphate (Schmidt, et al., 2012).

In contrast to widespread carbazole alkaloids from higher plants and fungi, bacterial carbazole metabolites are much less common. The first class of bacterial carbazoles are indolo[2,3- α]pyrrolo[3,4-*c*] carbazoles, representatives of which include staurosporine (Meksuriyen, et al., 1988) and rebeccamycin (Pearce et al., 1988), and the second class are indolosesequiterpenes, representatives of which are oridamycins (Takada, et al., 2010) and xiamycins (Ding, et al., 2010; Ding, et al., 2011). The bio-origins of both types of carbazole-containing metabolites have been well-established in the last decade (Howard-Jones et al., 2006; Xu, et al., 2012; Li et al., 2012; Li et al., 2015 and Baunach et al., 2015). The third type of carbazoles, however, consist of a simple tricyclic ring system with aliphatic side chains, including carquinostatins, carazostatin, carbazoquinocins, carbazomycin, (*S*)-streptovercillin and neocarazostatins (Feng, et al., 2007; Kato, et al., 1989; Kato, et al., 1991; Ruanpanun, et al., 2011; Sakano and Nakamura, 1980; Shin-ya, et al., 1993; Shin-ya, et al., 1997; Tanaka, et al., 1995) (Figure 1). Generally this group of bacterial carbazoles can act as free radical scavengers and exhibit potent neuronal cell protecting activity (Schmidt, et al., 2012). Free radicals play a key role in the initiation of a variety of diseases such as cerebral and myocardial ischemia, arteriosclerosis, inflammation, rheumatism and cancer. Antioxidants, acting as free radical scavengers, can act as protecting substances against damage caused by free radicals (Palinski, et al., 1989). In this respect, free radical scavenging compounds are being extensively investigated as potential drug leads (Schmidt, et al., 2012). Due to their pharmacological potential as cell protecting agents, there has been considerable interest for medicinal chemists to develop this class of molecules (Choshi, et al., 1997; Czerwonka, et al., 2006; Rawat and Wulff, 2004; Shin and Ogasawara, 1996). The biosynthetic pathways of this

group of bacterial carbazoles have not been reported although feeding experiments confirmed that L-tryptophan, pyruvate and acetate provide the carbazole nucleus (Kaneda, et al., 1990; Orihara, et al., 1997; Yamasaki, et al., 1983) (Figure S1A).

In our screening programme to discover novel natural products from the soil bacterium *Streptomyces sp.* MA37 (Deng, et al., 2014; Huang, et al., 2015; Ma, et al., 2015), neocarazostatin A **1** was isolated from this strain (Figure S1B-1G). Neocarazostatins A-C (Figure 1) were originally discovered from the culture of *Streptomyces sp.* GP38 in 1991 (Kato, et al., 1991). The neocarazostatins exhibited a strong inhibition effect on the free radical induced lipid peroxidation in rat brain homogenate. The IC₅₀ values of the neocarazostatins for inhibition of lipid peroxidation were considerably lower than those of the free radical scavenger butylhydroxytoluene (BHT) and brain protective agent flunarizine (Kato, et al., 1991).

In this study, we report the actinobacterial biosynthetic gene cluster for the biosynthesis of NZS. Two enzymes, NzsA and NzsG, were biochemically characterized. NzsA is a P450 hydroxylase and NzsG is a phytoene-synthase-like (PSL) prenyltransferase, a PSL protein that catalyses the prenylation of carbazole. Finally we reconstituted in vitro the last two steps of the pathway to NZS using purified recombinant enzymes.

Results and Discussion

Identification of the *nzs* gene cluster

NZS **1** possesses a prenyl group at C-6 on the indole ring. Initially, a homolog search of bacterial indole prenyltransferases was conducted. IptA from *Streptomyces sp.* SN-593 has been shown to be a 6-dimethyl-allyl (DMAL)-L-tryptophan synthase which is involved in the biosynthesis of 6-DMAL-3-carbaldehyde (Takahashi, et al., 2010). Although IptA homologs appeared to be widely spread in the *Streptomyces* genome, to our surprise, a BLAST search of the annotated genome of MA37 in the RAST server (Aziz, et al., 2008) yielded no ORFs with any obvious sequence identity to IptA in MA37.

Previous labelling studies established that indole pyruvate originating from L-tryptophan is likely to contribute rings B and C plus the intact C2 unit of C-3 and C-4 of ring A in the biosynthesis of carquinostatin B **3b** (Figure S1A) (Kato, et al., 1991), a structurally close

analogue of **1** (Figure 1). The incorporation of pyruvate in secondary metabolism can also be observed in the biosynthesis of sugars containing a two-carbon branched chain, such as antibiotic natural products, yersiniose A from the Gram-negative bacterium *Yersinia pseudotuberculosis*, (Chen, et al., 1998) aldgamycin E from *Saccharothrix* SA 103 (Ellestad, et al., 1967) and presumably tianchimycin B from *Saccharothrix xinjiangensis*. (Wang, et al., 2013). An *in vitro* assay indicated that the gene product YerE is a thiamine pyrophosphate (ThDP)-dependent enzyme, responsible for the C-C bond formation between 3-ketosugar and pyruvate during the biosynthesis of yersiniose A (Chen, et al., 1998; Lehwald, et al., 2010). We performed a homolog search of YerE in MA37, resulting in identification of an ORF, annotated as a ThDP-dependent enzyme (NzsH) (Figure 2A and Table 1), which shows moderate sequence identity (27%) to YerE.

Analysis of the genes in the close proximity of *nzsH* allowed us to retrieve a candidate gene cluster (*nzs*) spanning approximately 17.8 kb (Figure 2A and Table 1). The *nzs* cluster possesses 10 ORFs, 9 of which (NzsA-H and J) can be assigned catalytic functions (Table 1). A BLAST search of NzsI indicated that it belongs to a small group of hypothetical proteins with no obvious catalytic function. Genes beyond this region are highly conserved in the chromosomes of other non-NZS producing *Streptomyces* strains such as *S. griseus*, *S. avermitilis*, and *S. coelicolor* (Figure S2A). Thus, we propose that these 10 *orfs* define the boundaries of the *nzs* cluster.

***In vivo* experiments confirmed that the candidate gene cluster directs the biosynthesis of NZS 1**

To confirm the identity of the *nzs* cluster, gene disruption was performed and 10 different mutants ($\Delta nzsA-J$) were generated (Figure S2B-2L). HPLC analysis of the extracts from these mutants demonstrated that inactivation of *nzsE-F* and *nzsH-J* completely abolished the NZS production (Figure 2B), suggesting that these five ORFs are essential for the biosynthesis of **1**. Inactivation of *nzsB-D*, encoding anthranilate phosphoribosyltransferase, isopentenyl diphosphate (IPP) isomerase, and aromatic aminotransferase, respectively, resulted in only slightly decreased production of **1** (Figure 2B 5-8). In accordance with these findings, bioinformatics analyses of the draft genome sequence of the MA37 revealed the presence of

several other gene copies with predicted functions similar to NzsB-D, suggesting the cross-complementation roles played by these genes.

Gene disruption of *nzsG* completely abolished the production of **1** but resulted in accumulation of two new metabolites in the culture of the $\Delta nzsG$ mutant (Figure 2B 4). Subsequently fermentation and chemical isolation afforded two pure compounds, **4** (7 mg) and **5** (4.3 mg) (Figure 3). The structures of **4** and **5** were established by the inspection of HR-ESIMS and 1-D and 2-D NMR spectral data and by comparison of the NMR spectral data with those of **1** (Tables S4-5, Figure S3A-3F and Figure S3M-3R). Although compound **4** has identical chemical shifts in NMR spectra to the known carbazole metabolite, (*S*)-streptoverticillin, comparison of the values of the optical rotation of **4** with the ones of (*S*)-streptoverticillin and its non-natural enantiomer (*R*)-streptoverticillin (Thomas et al. 2011) indicated that **4** actually is (*R*)-streptoverticillin. Compound **5** is a new carbazole intermediate, which was named as precarazostatin. Both **4** and **5** lack prenyl substitution at C-6, suggesting that NzsG may be responsible for the prenylation at C-6 of the carbazole nucleus.

HPLC analysis also showed that, while the production of **1** was lost in the culture of the $\Delta nzsA$ mutant, two new metabolites, **2** and **6**, were accumulated (Figure 2B 2). Fermentation and isolation, followed by analyses of HR-ESIMS and 1-D and 2-D NMR spectral and optical rotation data established that one metabolite is a known carbazole metabolite, neocarazostatin B **2** (Figure 3, Figure S3G-3R) a close derivative of **1**, suggesting that NzsA may be responsible for the installation of the hydroxyl group at C-11 of **2** to generate **1**. The structure of compound **6** was determined as a new epoxy derivative of **2** on the basis of HR-ESIMS and 1- and 2-D NMR analyses, which clearly indicated the replacement of $\Delta^{16,17}$ in **2** with an epoxy ring (Figure 3 and Figure S3S-3X).

Biochemical assay demonstrated that NzsG is a new prenyltransferase that specifically acts on **5**

Given that **4** and **5** are not further metabolised in the $\Delta nzsG$ mutant, it was envisaged that they may be immediate substrates of NzsG. Bioinformatics analysis revealed that NzsG shares high sequence identity (60-65%) with only three hypothetical proteins from *Streptomyces* but has 25-40% similarity to a large family of putative phytoene synthases from actinomycetes. It also possesses a characteristic DDxxD motif which is essential for binding prenyl diphosphate

via metal ions (Liang, et al., 2002). However, NzsG shows no homology to the identified bacterial or fungi aromatic or indole PTases. Further phylogenetic analysis indicated that NzsG forms the same branch with phytoene synthases instead of all of the known aromatic or indole PTases (Figure S4A), implying that NzsG may be a new type of emerging PTase family.

To determine the exact function of NzsG, we carried out a biochemical study. Over-expression of *nzsG* in *E. coli* allowed isolation and purification of its encoded protein. The resultant NzsG appeared on SDS-PAGE with an estimated mol wt of 38.1 kDa (Figure S4B). Incubations of the recombinant enzyme with dimethylallyl pyrophosphate (DMAPP) and **4** or **5**, supplemented with Mg²⁺ (5 mM), were performed and the reactions were monitored by HPLC. When the assays were conducted in the absence of DMAPP or in the presence of **4**, there was no turnover (Figure 4). Reactions with **5**, however, resulted in an efficient conversion of **5** to neocarazostatin B **2** as evidenced by the exact mass and co-elution time with the authentic sample of **2** (Figure 4A-B and Figure S4C), confirming that **5** is the key intermediate in the NZS biosynthesis but its *bis*-methylated derivative, **4**, is a shunt product in the $\Delta nzsG$ mutant (Figure 4). The enzyme was found to have optimal activity at pH 8.0 at 30 °C in presence of Mg²⁺ (5mM) (K_m (**5**) = 202.5 ± 35.40, k_{cat} = 0.052 ± 0.004 min⁻¹) (Figure S4D-4F). There was no turnover when NzsG was incubated with DMAPP or FPP or indol derivatives (e.g. L-tryptophan, indole 3-pyruvate) or other tricyclic molecules (e.g. carbazole, acridine, fluorene, phenazine and dibenzothiophene, Figure 4 and Figure S4G-4H), suggesting that NzsG has restricted substrate specificity. It has been demonstrated that some fungal indol PTases possess substrate promiscuity and can be used to prenylate larger aromatic ring systems, i.e. indolocarbazoles, using chemoenzymatic approach (Yu, et al., 2012). NzsG, however, is the first native carbazole PTase reported and belongs to a new subgroup of aromatic PTases.

Biochemical assay demonstrated that NzsA is a P450 hydroxylase enzyme

Overexpression of *nzsA* in *E. coli* allowed isolation and purification of a soluble protein with an estimated mol wt 46.0 kDa, as observed in SDS-PAGE (Figure S5A). CO binding assay on NzsA monitored by UV spectroscopy demonstrated that NzsA is indeed a P450 enzyme (Figure S5B) (Meunier, et al., 2004). *In vitro* experiments showed that the recombinant enzyme efficiently converted **2** into **1** (Figure S5C) in the presence of NADPH (see supporting information). In control experiments, when assays were conducted in the absence of the

NADPH or the enzyme NzsA or in the presence of **6**, there were no turnovers (Figure 5), confirming that NzsA catalyses the installation of the hydroxyl group at C-11 position of **2** to yield **1** and the epoxy derivative **6** is a shunt product in the $\Delta nzsA$ mutant. NzsA was also incubated with (*R*)-streptovercillin **4** and precarazostatin **5**, but in both cases, no formation of a new product, or disappearance of the starting material, was observed (Figure 5). These observations strongly suggest that NzsA mediates the last enzymatic step in the biosynthesis of **1**.

To further confirm the biotransformation from **5** to **1** in the NZS biosynthesis, *in vitro* reconstituted biotransformation was carried out. Upon the incubation of **5** with the recombinant enzymes, NzsG and A, along with DMAPP, Mg^{2+} , and NADPH (see the supporting information), we observed the formation of **1** and **2** as evidenced by the exact mass and the same HPLC retention time as the authentic **1** and **2** (Figure S5D-5E).

Discussion

Based on the bioinformatics analysis and the experimental data, we propose the biosynthetic pathway of **1** in MA37 as shown in Scheme 1. NzsB-F are likely to be involved in the precursor pathways. NzsB could be a housekeeping enzyme for tryptophan supply. NzsD resembles a family of PLP-dependent aromatic amino acid aminotransferases, suggesting its role in the conversion of L-tryptophan to indole-3-pyruvic acid. NzsC, a putative type I isopentenyl diphosphate (IPP) isomerase, could be responsible for DMAPP supply (Berthelot, et al., 2012). NzsE is a putative acyl carrier protein (ACP), which presumably transfers malonyl-CoA into malonyl-ACP. Both NzsF and NzsJ are annotated as putative 3-oxoacyl-ACP synthases (KASIII). However, they share no significant sequence similarity with each other. While NzsJ bears no significant homology to characterized KAS III proteins, NzsF shares moderate sequence identity (37% identity and 55% similarity) to FabH from *Streptomyces coelicolor* A3(2) (Revill, et al., 2001), which catalyses the condensation reaction between acetyl-CoA and malonyl-ACP to form acetoacetyl-ACP. It is postulated that NzsF is responsible for the formation of acetoacetyl-ACP using acetyl-CoA and malonyl-ACP as substrates, followed by reduction to generate 3-hydroxy butyryl-ACP.

We propose that NzsH could perform an acyloin coupling reaction between indole 3-pyruvate and pyruvate to generate α -ketoacid intermediate **7**. The condensation reaction between **7**

and 3-hydroxy-butyryl-ACP could be mediated by the putative KASIII enzyme NzsJ via a reversible indole attack to yield **8**. Decarboxylation-driven cyclization of **8** would result in an indol-fused cyclopentane intermediate **9**, which could immediately undergo the ring rearrangement to generate an indol-fused cyclohexanone tricyclic intermediate **10**, followed by dehydration and hydroxylation at C4 of **10**, to generate **11**. **11** would be readily tautomerized using positively-charged nitrogen in the indole ring as the electron sink, followed by dehydration via base-catalyzed double-bond migration to furnish the *ortho*-quinone[*b*]indole tricyclic carbon backbone **12**. Examination of the metabolite profile extracted from the culture of the $\Delta nzsG$ mutant allowed identification of an ion with the identical *m/z* to **12** (Figure S6). Although this compound could not be isolated, the mass is consistent with the structure of the predicted intermediate **12**. The enzyme(s) responsible for the formation of **12** remain to be confirmed. The formation of **12** may partially resemble the enzymatic reaction catalysed by ScyC in the pathway of scytonemin (Balskus et al., 2009). The dimeric alkaloid scytonemin is a cyanobacterial metabolite, functioning as a sunscreen (Balskus et al., 2008). In case of scytonemin biosynthesis, ScyA, a ThDP-dependent enzyme, was found to be responsible for the acyloin coupling of indol-3-pyruvate and *p*-hydroxyphenylpyruvate to yield the β -ketoacid product (Balskus et al., 2008), which can then be cyclized and decarboxylated by the action of the unique enzyme, ScyC, to form the indole-fused cyclopentane intermediate (Balskus et al., 2009). It is hypothesized that NzsI could play a key role in this multistep biotransformation as our *in vivo* results indicated that *nzsI* is essential for the production of **1**. The exact roles of NzsH, J and I in the biosynthesis of **1** is currently under investigation in our labs. **12** could further undergo reduction, followed by *O*-methylation to yield the intermediate **5** and the shunt product streptoverillicin **4**. The prenylation event on **5** occurs in the presence of NzsG and DMAPP to produce **2**. The hydroxylation of **2** by NzsA finally provides **1**. Our *in vivo* and *in vitro* results unambiguously demonstrated the enzymatic coupled reactions from **5** to **1**, where the prenylation catalysed by NzsG must occur prior to the NzsA-mediated hydroxylation (Figures 4 and 5). When *nzsA* is inactivated, the $\Delta nzsA$ mutant also accumulates the epoxylated metabolite **6** via an unidentified epoxidase.

Significance

Neocarazostatin A **1** is a potent free scavenging agent for protecting cell damage caused by free radicals. It possesses an intriguing tricyclic aromatic ring system, of which the chemical logic during the biosynthesis remains to be determined. We describe here the identification and characterization of the gene cluster for NZS biosynthesis in the soil bacterium *Streptomyces* sp. MA37 through *in silico* analysis, gene inactivation and complementation. Biochemical assays of NzsG revealed that it is a new PSL-type carbazole prenyltransferase for NZS biosynthesis. *In vitro* assays confirmed that NzsA is responsible for the installation of a hydroxyl group at **2** to generate **1**. Finally we reconstituted the last two reactions tailoring the NZS biosynthesis and demonstrated the sequential enzymatic reaction catalysed by NzsG, followed by NzsA to transform the key intermediate **5** to **1**.

Materials and Methods

Media and strains used in this study

E. coli DH10B and *E. coli* ET12567 (pUZ802) were cultured in LB or LA medium at 37 °C. *Streptomyces* sp. MA37 was cultured in ISP2 medium (yeast extract 4 g/L, glucose 4 g/L, malt extract 10 g/L, pH 7.2), and modified ISP4 medium (10 g/L soluble starch, 2 g/L (NH₄)₂SO₄, 1 g/L K₂HPO₄, 1 g/L MgSO₄·7H₂O, 1 g/L NaCl, 1 g/L tryptone, 0.5 g/L yeast extract, 1 g/L peptone, trace element solution (1 mL/L), adjust pH to 7.2 before sterilization) containing the final concentration of 30 mM Mg²⁺ was used for conjugation of *Streptomyces* sp. MA37.

DNA sequencing and analysis

The open reading frames (ORFs) of the *nzs* gene cluster were deduced from the sequence by performing FramePlot 4.0 beta program (<http://nocardia.nih.go.jp/fp4/>). The corresponding deduced proteins were compared with other known proteins in the databases using the Basic Local Alignment Search Tool (BLAST) (<http://www.ncbi.nlm.nih.gov/blast/>). Amino acid sequence alignments were performed with the CLUSTALW algorithm from BIOLOGYWORKBENCH 3.2 software (<http://workbench.sdsc.edu>). The phylogenetic tree was drawn using MEGA 6.0 (Tamura., et al. 2013). The sequence of the neocarazostatin biosynthetic gene cluster was identified from the sequenced genome via BLAST method using YerE as the sequence query. The neocarazostatin biosynthetic gene cluster was submitted to NCBI GenBank with the accession number KP657980.

Extraction and purification of neocarazostatin A, neocarazostatin B, (*R*)-streptovercillin, precarazostatin and 16, 17-epoxyneocarazostatin B.

Streptomyces sp. MA37 and its mutants were inoculated into ISP2 medium, and were grown for two days at 28°C, 200 rpm. Then the culture was transferred into fresh ISP2 medium (1:100, volume to volume) and cultivated at 28°C, 200 rpm for 5 days. Mycelia were collected and re-suspended in one-tenth of the original culture volume of acetone, and the suspension was ultrasonically disrupted using KQ3200V Ultrasonic cleaning apparatus (40 kHz, 25 min). Cell pellets were eliminated by centrifugation and supernatant were subsequently dried out by rotary evaporation. Meanwhile the culture supernatant was extracted by an equal volume of ethyl acetate twice. The organic phase was collected and evaporated to dryness. Residues from two extracts were combined and re-dissolved in 1/100 of original culture volume of methanol for HPLC or LC-MS detection. Purification of the target compounds was performed by gel filtration (Sephadex G200) using methanol as the mobile phase. The corresponding sections were dried by rotary evaporation and dissolved in methanol, and were further purified by semi-preparative HPLC on an Agilent ZORBAX SB-C18 column (5 mm, 9.4x250 mm) at a flow rate of 3 mL/min. The wavelength of the UV monitor was set at 247 nm. For the detection of neocarazostatin A, the mobile phase was 52:48 A/B (solvent A was 0.1% formic acid in ultrapure water and solvent B was 0.1% formic acid in CH₃CN); for neocarazostatin B, the mobile phase was 42:58 A/B; for (*R*)-streptovercillin, the mobile phase was 45:55 A/B; for precarazostatin the mobile phase was 53:47 A/B; and for 16,17-epoxy-neocarazostatin B the mobile phase was 53:47 A/B. Finally, 10 mg of neocarazostatin A **1** ($[\alpha]_{D}^{19}$ -29 (c 0.07, MeOH)), 8.5 mg of neocarazostatin B **2** ($[\alpha]_{D}^{30}$ -28.8 (c 0.055, MeOH)), 7 mg of (*R*)-streptovercillin **4** ($[\alpha]_{D}^{30}$ -18.4 (c 0.84 MeOH)), and 4.3 mg of precarazostatin **5** ($[\alpha]_{D}^{31}$ -18.5 (c 0.07 MeOH)), 4.5 mg of $\Delta^{16,17}$ -epoxy-neocarazostatin B **6** ($[\alpha]_{D}^{30}$ -30.5 (c 0.34, MeOH)) were obtained.

HPLC MS/MS analysis

HPLC analysis was carried out on a DIKMA Diamonsil C18 column (250x4.6 mm, 5 μ m, column temperature 30°C) using a DIOEX P680 HPLC instrument. For fermentation analysis, samples were eluted with a gradient from 90:10 A/B to 60:40 A/B over 10 min, followed by another gradient to 45:55 A/B over 35 min at a flow rate of 1 mL/min, and UV monitor detected at

247 nm. For enzymatic analysis, samples were eluted with a gradient from 70:30 A/B to 0:100 A/B over 18 min, at a flow rate of 1 mL/min, and UV monitored at 247 nm. For carbazole, fluorene, phenazine, dibenzothiophene, acridine, Trp, IAA, IBA and indole-3-pyruvic acid, samples were eluted with a gradient from 95:5 A/B to 0:100 A/B over 25 min, at a flow rate of 1 mL/min, and UV monitored at 220 nm for carbazole, fluorene, phenazine, dibenzothiophene, 392 nm for acridine and 280 nm for Trp, IAA, IBA and indole-3-pyruvic acid. Twenty percent of the eluent was injected to source and eighty percent to waste during LC-MS analysis. Solvent A was 0.1% formic acid in ultrapure water and solvent B was 0.1% formic acid in CH₃CN. The same column and LC gradient was used in all LC-MS analysis. High resolution MS analysis, which consisted of a full scan in positive mode followed by a data dependent fragmentation scan, was performed on a Thermo Scientific LTQ XL Orbitrap mass spectrometer equipped with a Thermo Scientific Accela 600 pump.

NMR analysis

Nuclear magnetic resonance spectra of neocarazostatin B **2** (8.5 mg), (*R*)-streptovercillin **4** (7 mg), precarazostatin **5** (4.3 mg), and 16,17-epoxyneocarazostatin B **6** were recorded on Agilent 600 MHz instrument in CD₃OD. Nuclear magnetic resonance analyses of neocarazostatin A **1** were recorded on Varian 600 MHz spectrometer in CD₃Cl.

Structural elucidation of neocarazostatin A 1

HRESIMS analysis of **1** established a molecular formula of C₂₂H₂₇NO₄. Dereplication using Antibase (Laatsch, 2013) suggested that this compound could be a known metabolite, neocarazostatin A, previously isolated from *Streptomyces sp.* GP38 (Kata, et al., 1991). **1** also showed a characteristic UV pattern, with absorption maxima at 229, 249, 271, 292, 331 and 345 nm. To confirm the structure, a complete set of 1D and 2D NMR spectral data was obtained. The structure of **1** was finally established through comparison of ¹H and ¹³C NMR spectra data with those previously reported which unambiguously confirms that **1** is neocarazostatin A.

In-frame deletion of *nzsA* to *nzsH*

To inactivate *nzsA*, a 2030 bp upstream fragment and a 2002 bp downstream fragment were amplified from genomic DNA of *Streptomyces* sp. MA37 by PCR using the primers N-2-up-F/N-2-up-R and N-2-do-F/N-2-do-R respectively (Table S3). PCR was performed in 20 μ L volume with 5% DMSO and KOD DNA polymerase (TOYOBO). The amplification conditions were: initial denaturation at 95 °C for 5 min; 30 cycles of denaturation at 95 °C for 30 s, annealing at 58 °C for 30 s, and extension at 68 °C for 2 min; and gap infilling at 68°C for 10 min. The obtained fragments were cloned into the HindIII/EcoRI site of pKC1139 by using In-fusion[®] HD Cloning Kit (Clontech) to obtain the in-frame deletion vector construct, which was then transferred into *Streptomyces* sp. MA37 via *E. coli-Streptomyces* conjugation. Following a previously-published procedure (Yu et al., 2009), the *nzsA* in-frame deletion mutant strains were identified by screening out and designated as WDY633. The same strategy was used to construct *nzsB* to *nzsJ* in-frame deletion mutants, except that different primers were used to amplify the left and right arms of the target genes (Table S3). The in-frame deletion mutant strains of *nzsB* to *NzsJ* were designated as WDY640, WDY641, WDY642, WDY644, WDY646, WDY638, WDY630, WDY648, and WDY635 respectively (Table S1).

Complementation of the mutant strain WDY633, WDY644, WDY646, WDY638, WDY630, WDY648 and WDY635

To complement WDY633, a 1257 bp fragment that contains the whole *nzsA* gene sequence was amplified from genomic DNA of *Streptomyces* sp. MA37 by high fidelity PCR using the primers N-1-HB-F/N-1-HB-R (Table S3). The amplification conditions were: initial denaturation at 95 °C for 5 min; 30 cycles of denaturation at 95 °C for 30 s, annealing at 58 °C for 30 s, and extension at 68 °C for 1 min; and gap infilling at 68°C for 10 min. The obtained fragment was cloned into the NdeI/EcoRI site of pIB139, which can integrate into *Streptomyces* chromosome via Φ C31 phage site. The construct obtained was then transferred into *Streptomyces* sp. MA37 in-frame deletion mutant via *E. coli-Streptomyces* conjugation. Followed the procedure described previously (Kieser et al., 2000), the Δ *nzsA* complementation mutant strain was identified by screening out and designated as WDY634. The same strategy was used to complement WDY644, WDY646, WDY638, WDY630, WDY648, and WDY635, except that different pairs of primers were used for each complementation construct (Table S3). The complementation mutant strains of Δ *nzsB*, Δ *nzsE*, Δ *nzsF* and Δ *nzsG*-

J were identified by screening out and designated as WDY638, WDY647, WDY639, WDY631, WDY649 and WDY636 respectively.

Construction of NzsA and NzsG overexpression vector

To overexpress NzsA, a 1257 bp fragment that contains the whole *nzsA* was amplified from genomic DNA of *Streptomyces* sp. MA37 by PCR using the primers NzsA_F/NzsA_R (Table S3). PCR was performed in 20 μ L volume with 5% DMSO and KOD DNA polymerase (TOYOBO). The amplification conditions were: initial denaturation at 95 °C for 5 min; 30 cycles of denaturation at 95 °C for 30 s, annealing at 58 °C for 30 s, and extension at 68 °C for 90 s; and gap infilling at 68°C for 10 min. The obtained fragments were cloned into the KpnI/XhoI site of pHS_SUMO (Lv, et al., 2015) by using In-fusion HD Cloning Kit (Clontech) to yield the overexpression construct pWDY651. The same strategy was used for *nzsG* cloning, except that the primers NzsG_F/NzsG_R were used for amplification (Table S3). The NzsG overexpression construct was designated pWDY650.

Expression and purification of NzsA and NzsG

The protein expression constructs pWDY638 and pWDY639 were individually transformed into *E. coli* BL21 (IDE3) (Novagen) competent cells. Single colonies from each transformation were inoculated to a starter culture (5 mL SOB media containing 50 μ g/mL kanamycin) and cultivated at 37 °C and 200 rpm. When the A600 of the medium reached 0.5, the culture was transferred to 500 mL of fresh SOB medium and incubated at 37 °C, 200 rpm. IPTG was added to a final concentration of 1 mM when the A600 reached 0.6. After overnight culture at 16 °C, cells were harvested by centrifugation and frozen at -40 °C. All subsequent steps were performed at 4 °C. After thawed on ice, cells were suspended in lysis buffer (200 mM Tris-HCl, pH 8.0, 500 mM NaCl, 10 mM imidazole). The cell suspension was lysed with a Nano Homogenize Machine (ATS Engineering Inc, AH100B). To separate the cellular debris from the soluble protein, the lysate was centrifuged at 20,000 x g, 4 °C for 20 min. The supernatant was incubated with 1.5 mL Ni Sepharose™ 6 Fast Flow (GE Healthcare) which had been pre-equilibrated with equilibration buffer (200 mM Tris-HCl (pH 8.0), 500 mM NaCl, and 10 mM imidazole) for 2 h at 4 °C. The resin was washed with 5 mL of the equilibration buffer, followed by then twice with buffer containing 25 mM imidazole. The recombinant protein was eluted with 5 mL wash buffer containing 250 mM imidazole. The eluted recombinant proteins were

concentrated to 2.5 mL using Centrifugal Filter Units (Milipore, Regenerated Cellulose 3,000 MWCO). Then the samples were desalted by PD-10 Columns (GE Healthcare) according to manufacture instruction. The cleavage of the SUMO tag of the eluted recombinant proteins was conducted by using SUMO Protease (Invitrogen, Catalog no. 12588-018) in the buffer composed of 50 mM Tris-HCl, pH 8.0, and 150 mM NaCl at 4 °C for 4 h. The SUMO tag and SUMO Protease were finally removed from the cleavage reaction by using 0.5 mL Ni Sepharose™ 6 Fast Flow (GE Healthcare). The purified protein was stored at -80 °C in storage buffer (50mM Tris-HCl, pH 8.0, 150mM NaCl, 10% (w/v) glycerol, 1mM DTT).

NzsG activity assay

The enzyme assay of NzsG was carried out in 50 mM Tris-HCl buffer (pH 7.5) with 5 mM MgCl₂, containing 0.8 mg/mL NzsG, 1 mM substrate and 0.2 mM DMAPP, in a final volume of 50 µL. The optimal assay conditions were obtained at 30 °C. After 30 min, the reaction was quenched by the addition of two equal volume of methanol and mixed by vortexing. The mixture was centrifuged at 15,000 rpm for 20 min to remove protein. The supernatant was then subjected to LC-MS/MS analysis under the same conditions as described above.

Kinetic studies of NzsG

Optimization of NzsG *in vitro* assays is described in the Figure S4D legend. The enzyme assays of NzsG were performed in a total volume of 50 µL mixture containing 50 mM Tris-HCl (pH 8.0), 5 mM Mg²⁺, 1 mM DMAPP, 1 mM DTT and 0.087 mM to 3 mM precarazostatin 5 at 30 °C for 10 min. Reactions were initiated by the addition of enzyme (0.5 µM NzsG). An equal volume of methanol to quench the reaction and to remove proteins by centrifugation. The supernatant was analyzed by HPLC. Kinetic analyses of NzsG reactions were carried out as described in the Figure S4F legend

NzsA activity assay

Enzyme assay of NzsA activity was carried out on a 50 µL scale with substrates (1 mM), NzsA (1mg/mL), spinach ferredoxin (100 µg/mL), spinach ferredoxin-NADP⁺ reductase (0.2 U/mL), NADPH (1.0 mM), glucose-6-phosphate (10 mM), and glucose-6-phosphate dehydrogenase (10 U/mL) in Tris-HCl buffer (50 mM, pH 7.5). After incubated at 30 °C for 30 min, the reaction

was quenched by the addition of two equal volume of methanol and mixed by vortexing. The mixture was centrifuged at 15,000 rpm for 20 min to remove protein. The supernatant was then subjected to LC-MS/MS analysis under the same conditions as described above.

Acknowledgements

Y.Y. thanks the financial support from "973" Program (2012CB721006) and National Natural Science Foundation of China (31570033). RE, KK, HD and MJ acknowledge the financial supports of the Leverhulme Trust-Royal Society Africa Award (AA090088). The sequence of the *nzs* gene cluster from *Streptomyces* sp. MA37 has been deposited in Genbank database under the accession no. KP657980. There is no conflict of interest to declare.

References

- Aziz, R.K., Bartels, D., Best, A.A., DeJongh, M., Disz, T., Edwards, R.A., Formsma, K., Gerdes, S., Glass, E.M., and Kubal, M. (2008). The RAST Server: rapid annotations using subsystems technology. *BMC Genomics* 9, 75.
- Balskus, E. P. and Walsh, C. T. (2008). Investigating the initial steps in the biosynthesis of cyanobacterial sunscreen scytonemin. *J. Am. Chem. Soc.* 130, 15260-15261.
- Balskus, E. P. and Walsh, C. T. (2009). An enzymatic cyclopentyl[b]indole formation involved in scytonemin biosynthesis. *J. Am. Chem. Soc.* 131, 14648-14649.
- Baunach, M. Ding, L., Willing, K., Hertweck, C. (2015). Bacterial synthesis of unusual sulfonamide and sulfone antibiotics by flavoenzyme-mediated sulfur dioxide capture. *Angew. Chem. Int. Ed.* DOI: 10.1002/anie.201506541
- Berthelot, K., Estevez, Y., Deffieux, A., and Peruch, F. (2012). Isopentenyl diphosphate isomerase: A checkpoint to isoprenoid biosynthesis. *Biochimie* 94, 1621-1634.
- Chen, H., Guo, Z., and Liu, H.-w. (1998). Biosynthesis of yersiniose: attachment of the two-carbon branched-chain is catalyzed by a thiamine pyrophosphate-dependent flavoprotein. *J. Am. Chem. Soc.* 120, 11796-11797.
- Choshi, T., Sada, T., Fujimoto, H., Nagayama, C., Sugino, E., and Hibino, S. (1997). Total syntheses of carazostatin, hyellazole, and carbazoquinocins BF. *J. Org. Chem.* 62, 2535-2543.
- Czerwonka, R., Reddy, K.R., Baum, E., and Knölker, H.-J. (2006). First enantioselective total synthesis of neocarazostatin B, determination of its absolute configuration and transformation into carquinostatin A. *Chem. Commun.*, 711-713.
- Deng, H., Ma, L., Bandaranayaka, N., Qin, Z., Mann, G., Kyeremeh, K., Yu, Y., Shepherd, T., Naismith, J.H., and O'Hagan, D. (2014). Identification of fluorinases from *Streptomyces* sp MA37, *Nocardia brasiliensis*, and *Actinoplanes* sp N902-109 by genome mining. *ChemBioChem* 15, 364-368.
- Ding, L.; Münch, J.; Goerls, H.; Maier, A.; Fiebig, H.-H.; Lin, W.-H.; Hertweck, C. (2010). Xiamycin, a pentacyclic indolosesquiterpene with selective anti-HIV activity from a bacterial mangrove endophyte. *Bioorg. Med. Chem. Lett.* 20, 6685-7.
- Ding, L.; Maier, A.; Fiebig, H.-H.; Lin, W.-H.; Hertweck, C. (2011). A family of multicyclic indolosesquiterpenes from a bacterial endophyte. *Org. Biomol. Chem.* 9, 4029-31.
- Ellestad, G., Kunstmann, M., Lancaster, J., Mitscher, L., and Morton, G. (1967). Structures of methyl alldgarosides A and B obtained from the neutral macrolide antibiotic alldgamycin E. *Tetrahedron* 23, 3893-3902.
- Feng, N., Ye, W.H., Wu, P., Huang, Y.C., Xie, H.H., and Wei, X.Y. (2007). Two new antifungal alkaloids produced by *Streptoverticillium morookaense*. *J. Antibiot.* 60, 179-183.

Howard-Jones, A. R.; Walsh, C. T. (2006). Staurosporine and Rebeccamycin Aglycones Are Assembled by the Oxidative Action of StaP, StaC, and RebC on Chromopyrrolic Acid. *J. Am. Chem. Soc.* 2006, 128, 12289-12298.

Huang, S., Tabudravu, J., Elsayed, S.S., Travert, J., Peace, D., Tong, M.H., Kyeremeh, K., Kelly, S.M., Trembleau, L., Ebel, R., Jaspars, M., Yu, Y., Deng, H. (2015). Discovery of a Single Monooxygenase that Catalyzes Carbamate Formation and Ring Contraction in the Biosynthesis of the Legonmycins. *Angew. Chem. Int. Ed. Engl.* 54, 12697-12701.

Kaneda, M., Kitahara, T., Yamasaki, K., and Nakamura, S. (1990). Biosynthesis of Carbazomycin-B .2. Origin of the Whole Carbon Skeleton. *J. Antibiot.* 43, 1623-1626.

Kato, S., Kawai, H., Kawasaki, T., Toda, Y., Urata, T., and Hayakawa, Y. (1989). Studies on free radical scavenging substances from microorganisms. I. Carazostatin, a new free radical scavenger produced by *Streptomyces chromofuscus* DC 118. *J Antibiot (Tokyo)* 42, 1879-1881.

Kato, S., Shindo, K., Kataoka, Y., Yamagishi, Y., and Mochizuki, J. (1991). Studies on free radical scavenging substances from microorganisms. II. Neocarazostatins A, B and C, novel free radical scavengers. *J Antibiot (Tokyo)* 44, 903-907.

Kieser T., Bibb M.J., Buttner M.J., Chater K.F., Hopwood D.A. (2000) *Practical Streptomyces Genetics*, UK: The John Innes Foundation Norwich.

Knölker, H.J., and Reddy, K.R. (2002). Isolation and synthesis of biologically active carbazole alkaloids. *Chem. Rev.* 102, 4303-4427.

Laatsch, H. *AntiBase 2013: The Natural Compound Identifier. WILEY-VCH* (2013).

Lehwald, P., Richter, M., Röhr, C., Liu, H.w., and Müller, M. (2010). Enantioselective Intermolecular Aldehyde – Ketone Cross - Coupling through an Enzymatic Carboligation Reaction. *Angew. Chem. Int. Ed.* 49, 2389-2392.

Li, H., Zhang, Q., Li, S., Zhu, Y., Zhang, G., Zhang, H., Tian, X., Zhang, S., Ju, J., Zhang, C. (2012). Identification and Characterization of Xiamycin A and Oxiamycin Gene Cluster Reveals an Oxidative Cyclization Strategy Tailoring Indolosesquiterpene Biosynthesis. *J. Am. Chem. Soc.* 2012, 134, 8996 – 9005;

Li, H., Sun, Y., Zhang, Q., Zhu, Y. Li, S. M., A. Li, Zhang, C. (2015). Elucidating the Cyclization Cascades in Xiamycin Biosynthesis by Substrate Synthesis and Enzyme Characterizations. *Org. Lett.* 17, 306 – 309;

Li, L., Xu, Z., Xu, X., Wu, J., Zhang, Y., He, X., Zabriskie, T. M., Deng, Z. (2008). The Mildiomycin Biosynthesis: Initial Steps for Sequential Generation of 5-Hydroxymethylcytidine 5'-Monophosphate and 5-Hydroxymethylcytosine in *Streptovorticillium rimofaciens* ZJU5119. *ChemBioChem.* 9, 1286-1294.

Liang, P.H., Ko, T.P., and Wang, A.H.J. (2002). Structure, mechanism and function of prenyltransferases. *Eur. J. Biochem.* 269, 3339-3354.

Ma, L., Bartholome, A., Tong, M.H., Qin, Z., Yu, Y., Shepherd, T., Kyeremeh, K., Deng, H., and O'Hagan, D. (2015). Identification of a fluorometabolite from *Streptomyces* sp. MA37:(2 R 3 S 4 S)-5-fluoro-2, 3, 4-trihydroxypentanoic acid. *Chem. Sci.* 6, 1414-1419.

Lv, M., Zhao, J., Deng, Z., Yu, Y. (2015). Characterization of the Biosynthetic Gene Cluster for Benzoxazole Antibiotics A33853 Reveals Unusual Assembly Logic. *Chem. Bio.* 22, 1313 - 1324.

Meksuriyen, D.; Cordell, G. A. (1988). Biosynthesis of Staurosporine, 1. 1H- and 13C-nmr Assignments. *J. Nat. Prod.*, 51, 884-892

Meunier, B., De Visser, S.P., and Shaik, S. (2004). Mechanism of oxidation reactions catalyzed by cytochrome P450 enzymes. *Chem. Rev.* 104, 3947-3980.

Orihara, N., Furihata K., Seto, H. (1997). Studies on the biosynthesis of terpenoidal compounds produced by actinomycetes, 2. Biosynthesis of carquinostatin B via the non-mevalonate pathway in *Streptomyces exfoliates*,. *J Antibiotics* 50, 979-981.

Palinski, W., Rosenfeld, M.E., Ylaherttua, S., Gurtner, G.C., Socher, S.S., Butler, S.W., Parthasarathy, S., Carew, T.E., Steinberg, D., and Witztum, J.L. (1989). Low-Density Lipoprotein Undergoes Oxidative Modification In vivo. *PNAS* 86, 1372-1376.

Pearce, C. J.; Doyle, T. W.; Forenza, S.; Lam, K. S.; Schroeder, D. R. (1988). The biosynthetic origin of rebeccamycin. *J. Nat. Prod.*, *51*, 937-940.

Rawat, M., and Wulff, W.D. (2004). Total synthesis of carbazoquinocin C: application of the o-benzannulation of Fischer carbene complexes to carbazole-3, 4-quinone alkaloids. *Org. Lett.* *6*, 329-332.

Revill, W.P., Bibb, M.J., Scheu, A.K., Kieser, H.J., and Hopwood, D.A. (2001). Beta-ketoacyl acyl carrier protein synthase III (FabH) is essential for fatty acid biosynthesis in *Streptomyces coelicolor* A3(2). *J. Bacteriol.* *183*, 3526-3530.

Ruanpanun, P., Dame, Z.T., Laatsch, H., and Lumyong, S. (2011). 3-Methoxy-2-methyl-carbazole-1,4-quinone, carbazomycins D and F from *Streptomyces* sp. CMU-JT005. *FEMS Microbiol. Lett.* *322*, 77-81.

Sakano, K., and Nakamura, S. (1980). New antibiotics, carbazomycins A and B. II. Structural elucidation. *J Antibiot (Tokyo)* *33*, 961-966.

Schmidt, A.W., Reddy, K.R., and Knölker, H.J. (2012). Occurrence, biogenesis, and synthesis of biologically active carbazole alkaloids. *Chem. Rev.* *112*, 3193-3328.

Shin-ya, K., Tanaka, M., Furihata, K., Hayakawa, Y., and Seto, H. (1993). Structure of carquinostatin A, a new neuronal cell protecting substance produced by *Streptomyces exfoliatus*. *Tetrahedron Lett.* *34*, 4943-4944.

Shin-ya, K., and Ogasawara, K. (1996). Enantiotopical Synthesis of Carbazoquinocins A and D, The Potent Lipid Peroxidation Inhibitors from *Streptomyces violaceus* 2448-SVT2. *Synlett*, 922-924.

Shinya, K., Kunigami, T., Kim, J.S., Furihata, K., Hayakawa, Y., and Seto, H. (1997). Carquinostatin B, a new neuronal cell-protecting substance produced by *Streptomyces exfoliatus*. *Biosci. Biotechnol., Biochem.* *61*, 1768-1769.

Takada, K.; Kajiwaru, H.; Imamura, N. (2010). Oridamycins A and B, anti-Saprolegnia parasitica indolosesquiterpenes isolated from *Streptomyces* sp. KS84. *J. Nat. Prod.* *73*, 698-701.

Takahashi, S., Takagi, H., Toyoda, A., Uramoto, M., Nogawa, T., Ueki, M., Sakaki, Y., and Osada, H. (2010). Biochemical characterization of a novel indole prenyltransferase from *Streptomyces* sp. SN-593. *J. Bacteriol.* *192*, 2839-2851.

Tamura, K., Stecher, G., Peterson, D., Filipski, A., Kumar, S. (2013). MEGA6: Molecular Evolutionary Genetics Analysis version 6.0. *Mol. Biol. Evol.* *30*, 2725-2729.

Tanaka, M., Shin-ya, K., Furihata, K., and Seto, H. (1995). Isolation and structural elucidation of antioxidative substances, carbazoquinocins A to F. *J Antibiot (Tokyo)* *48*, 326-328.

Thomas C., Kataeva O., Knölker H. J. (2011). Transition metals in organic synthesis, part 96. first total synthesis of streptovercillin: unambiguous confirmation of the absolute configuration. *Synlett.* *18*, 2663-2666.

Wang, X., Tabudravu, J., Jaspars, M., and Deng, H. (2013). Tianchimycins A–B, 16-membered macrolides from the rare actinomycete *Saccharothrix xinjiangensis*. *Tetrahedron* *69*, 6060-6064.

Xu, Z., Baunach, M., Ding, L., Hertweck, C. (2012). Bacterial Synthesis of Diverse Indole Terpene Alkaloids by an Unparalleled Cyclization Sequence. *Angew. Chem. Int. Ed.* *2012*, *51*, 10293 – 10297;

Yamasaki, K., Kaneda, M., Watanabe, K., Ueki, Y., Ishimaru, K., Nakamura, S., Nomi, R., Yoshida, N., and Nakajima, T. (1983). New Antibiotics, Carbazomycin-a and Carbazomycin-B .3. Taxonomy and Biosynthesis. *J. Antibiot.* *36*, 552-558.

Yu, X., Liu, Y., Xie, X., Zheng, X.D., and Li, S.M. (2012). Biochemical characterization of indole prenyltransferases: filling the last gap of prenylation positions by a 5-dimethylallyltryptophan synthase from *Aspergillus clavatus*. *J. Biol. Chem.* *287*, 1371-1380.

Yu, Y., Duan, L., Zhang, Q., Liao, R., Ding, Y., Pan, H., Wendt-Pienkowski, E., Tang, G., Shen, B., Liu, W. (2009). Nosiheptide biosynthesis featuring a unique indole side ring formation on the characteristic thiopeptide framework. *ACS Chem. Biol.* *4*, 855-864.

Figure 1. Chemical structures of common tricyclic carbazole alkaloids from bacteria

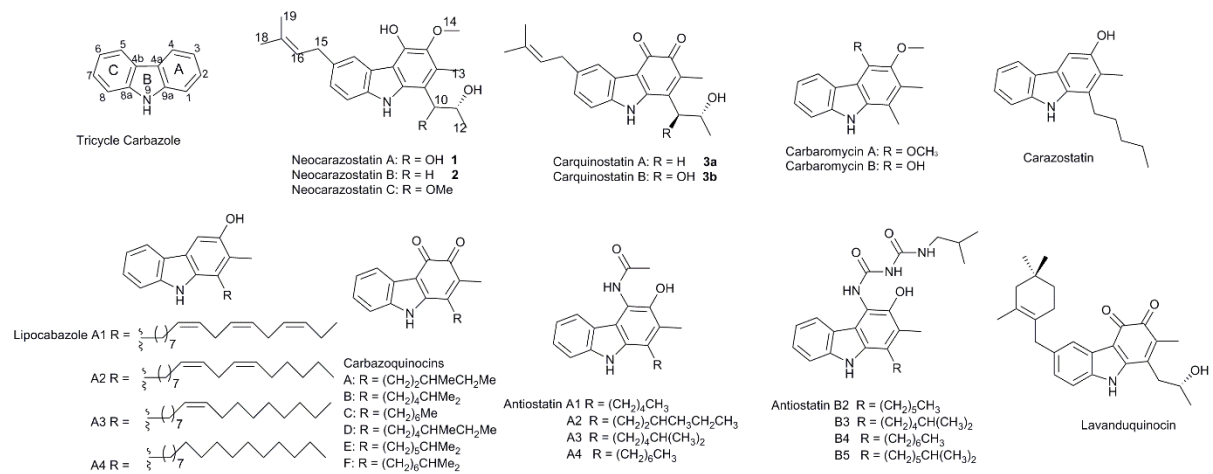


Figure 2 A. Genetic organization of the *nzs* biosynthetic gene cluster. Blue: the genes putatively involved in the biosynthesis of 1. Red: genes involved in the biosynthesis of indole-3-pyruvate precursor; Yellow: genes involved in the biosynthesis of DMAPP precursor; Purple: genes putatively involved in the PKS biosynthesis; Grey: gene with unknown function. **B.** HPLC analyses (UV at 247nm) of extracts from the *Streptomyces* sp. MA37 wild type and mutant strains. **1** and **10**: wild type strain; **2**: WDY633 ($\Delta nzsA$ mutant); **3**: WDY634 ($\Delta nzsA$ complementation mutant); **4**: WDY638 ($\Delta nzsG$ mutant); **5**: WDY639 ($\Delta nzsG$ complementation mutant); **6**: WDY640 ($\Delta nzsB$ mutant); **7**: WDY641 ($\Delta nzsC$ mutant); **8**: WDY642 ($\Delta nzsD$ mutant); **9**: WDY644 ($\Delta nzsE$ mutant); **11**: WDY645 ($\Delta nzsE$ complementation mutant); **12**: WDY646 ($\Delta nzsF$ mutant); **13**: WDY647 ($\Delta nzsF$ complementation mutant); **14**: WDY630 ($\Delta nzsH$ mutant); **15**: WDY631 ($\Delta nzsH$ complementation mutant); **16**: WDY648 ($\Delta nzsI$ mutant); **17**: WDY649 ($\Delta nzsI$ complementation mutant); **18**: WDY635 ($\Delta nzsJ$ mutant); **19**: WDY636 ($\Delta nzsJ$ complementation mutant).

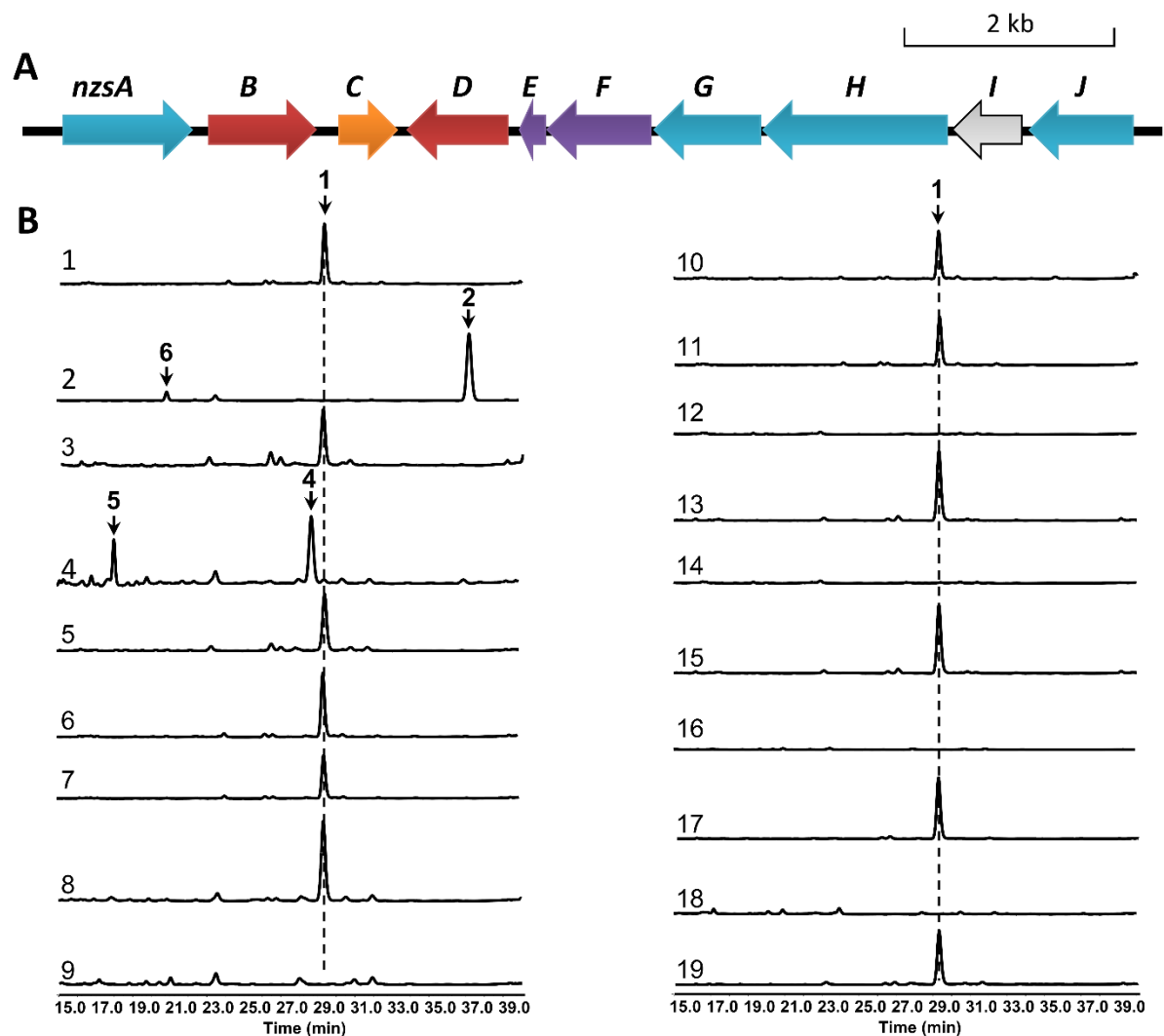


Table 1. Deduced functions of ORFs in *nzs* biosynthetic gene cluster

gene	size ^a	Protein homolog (accession no.), origin	I/S ^b	proposed function
<i>nzsA</i>	418	Cytochrome P450 monooxygenase (CBX53644), <i>S. platensis</i> NRRL 2364	34/51	Hydroxylation
<i>nzsB</i>	355	Anthranilate phosphoribosyltransferase (AIR97966), <i>S. glaucescens</i>	79/88	Tryptophan biosynthesis
<i>nzsC</i>	185	isopentenyl-diphosphate delta-isomerase (KES08965), <i>S. toyocaensis</i>	72/77	IPP isomerase
<i>nzsD</i>	325	phenylalanine aminotransferase (AIR99319), <i>S. glaucescens</i>	46/61	Aminotransferase
<i>nzsE</i>	80	acyl carrier protein(WP_030783257), <i>S. lavenduligriseus</i>	62/77	ACP
<i>nzsF</i>	337	FabH (CAB62720), <i>S. coelicolor</i> A3(2)	37/55	KAS III
<i>nzsG</i>	334	phytoene synthase CrtB (AAG28701), <i>S. griseus</i> IFO13350	28/40	Isoprenyl transferase
<i>nzsH</i>	593	acetolactate synthase YerE (AEP25490), <i>Yersinia pseudotuberculosis</i>	27/41	Acetolactate synthase
<i>nzsI</i>	227	hypothetical protein (WP_030783270), <i>S. lavenduligriseus</i>	80/88	Unknown function
<i>nzsJ</i>	331	3-oxoacyl-ACP synthase OleA (ACS30828), <i>Micrococcus luteus</i> NCTC 2665	24/35	KAS III

^a amino acids. ^b Identity/Similarity

Figure 3. Chemical structures of intermediates and shunt products isolated from the mutants in this study. The structures of **2**, **4-6** were fully characterized by HR-ESIMS and 1- and 2-D NMR spectroscopic analyses

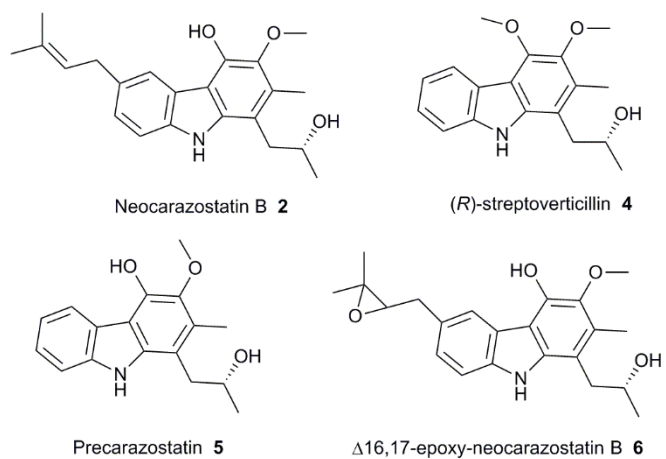


Figure 4. HPLC analysis (UV at 247 nm) of the reactions catalysed by NzsG. Trace A. standard **5**; Trace B shows the analysis of the conversion of **5** to **2** in a reaction containing Mg^{2+} (5mM), **5** (1mM), NzsG (0.8 mg/mL) and DMAPP (0.2 mM); Traces C-F show the analyses of reactions containing Mg^{2+} (5 mM), NzsG (0.8 mg/mL) and various substrates, indicating that only **5** is the substrate for NzsG.

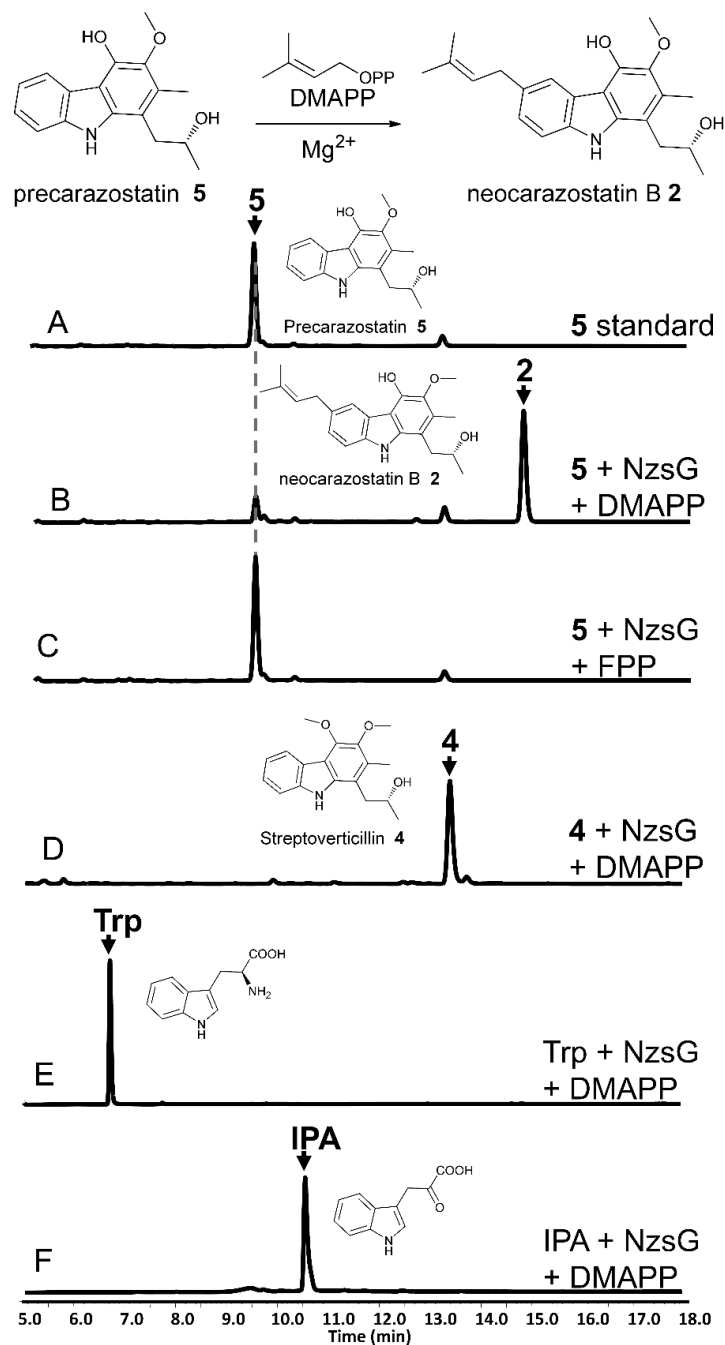
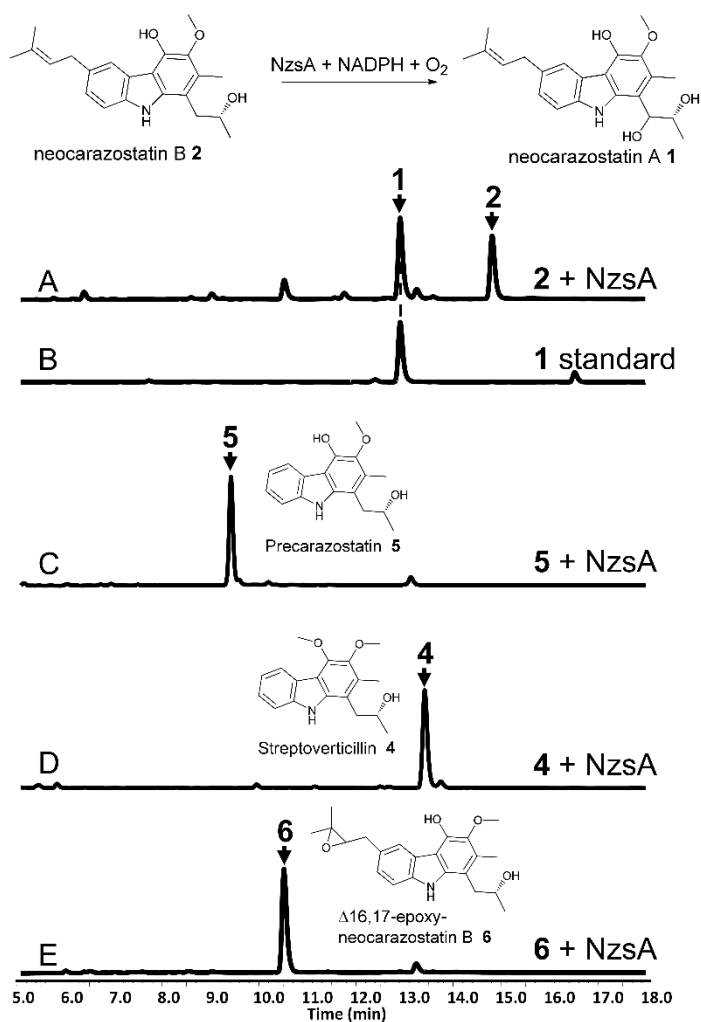


Figure 5. HPLC analysis (UV at 247 nm) of the biochemical reactions in presence of NzsA. Trace A shows the analysis of the conversion of **2** to **1** in a reaction containing **2** (1 mM), NzsA (1mg/mL), spinach ferredoxin (100 μ g/mL), spinach ferredoxin-NADP+ reductase (0.2 U/mL), NADPH (1.0 mM), glucose-6-phosphate (10 mM), and glucose-6-phosphate dehydrogenase (10 U/mL) in a Tris-HCl buffer (50 mM, pH 7.5). Trace B shows the standard **2**; Traces C-E show the analyses of reactions containing NADPH, NzsA (1 mg/mL) and various substrates, indicating that only **2** is the substrate for NzsA.



Scheme 1 A. Proposed model for indole-3-pyruvate; **B.** the biosynthesis of DMAPP; **C.** the biosynthesis of 3-hydroxy-butryl-ACP; **D.** Proposed biosynthetic pathway of **1**. Bracket: **9** was observed to be present in the extract of the mutant $\Delta nzsG$ based on HR-ESIMS and MSⁿ analyses. Dashed line: proposed reactions. Solid line: reactions were confirmed biochemically.

